Applied and Environmental Microbiology, Mar. 2010, p. 1935–1945 Vol. 76, No. 6
0099-2240/10/$12.00 doi:10.1128/AEM.02323-09

Functional Genomic Study of Exogenous *n*-Butanol Stress in *Escherichia coli*▽†‡

Becky J. Rutherford,[1,2] Robert H. Dahl,[1,2] Richard E. Price,[4] Heather L. Szmidt,[2,5] Peter I. Benke,[2,5] Aindrila Mukhopadhyay,[2,5]* and Jay D. Keasling[1,2,3,5]

Department of Chemical Engineering, University of California, Berkeley, California 94720[1]; Joint BioEnergy Institute, Emeryville, California 94608[2]; Department of Bioengineering, University of California, Berkeley, California 94720[3]; Department of Molecular and Cellular Biology, University of California, Berkeley, California 94720[4]; and Physical Biosciences Division, Lawrence Berkeley National Laboratory, Berkeley, California 94720[5]

Received 25 September 2009/Accepted 16 January 2010

***n*-Butanol has been proposed as an alternative biofuel to ethanol, and several industrially used microbes, including *Escherichia coli*, have been engineered to produce it. Unfortunately, *n*-butanol is more toxic than ethanol to these organisms. To understand the basis for its toxicity, cell-wide studies were conducted at the transcript, protein, and metabolite levels to obtain a global view of the *n*-butanol stress response. Analysis of the data indicates that *n*-butanol stress has components common to other stress responses, including perturbation of respiratory functions (*nuo* and *cyo* operons), oxidative stress (*sodA*, *sodC*, and *yqhD*), heat shock and cell envelope stress (*rpoE*, *clpB*, *htpG*, *cpxR*, and *cpxP*), and metabolite transport and biosynthesis (*malE* and *opp* operon). Assays using fluorescent dyes indicated a large increase in reactive oxygen species during *n*-butanol stress, confirming observations from the microarray and proteomics measurements. Mutant strains with mutations in several genes whose products changed most dramatically during *n*-butanol stress were examined for increased sensitivity to *n*-butanol. Results from these analyses allowed identification of key genes that were recruited to alleviate oxidative stress, protein misfolding, and other causes of growth defects. Cellular engineering based on these cues may assist in developing a high-titer, *n*-butanol-producing host.**

Short-chain alcohols such as propanol, butanol, and pentanol have recently been highlighted as potential transportation fuels with many advantages over ethanol, and several new studies have focused on the microbial production of these alcohols (24). Among these, *n*-butanol has gained popularity as an alternative fuel since it can be blended with gasoline, is compatible with existing supply infrastructure, and has higher energy content than ethanol (14). However, *n*-butanol accumulation is also known to be highly toxic to native producers (e.g., *Clostridium*) and engineered hosts (e.g., *Escherichia coli*) (6, 27). As such, it is difficult to produce *n*-butanol at the titers needed for economic efficiency.

Understanding the stress response of potential *n*-butanol-producing microorganisms could facilitate engineering them for improved tolerance. In the absence of a high-titer, *n*-butanol-producing host, *n*-butanol can be added exogenously to cultures in order to elucidate the stress response. In this study, we used functional genomics (microarrays, proteomics, and targeted metabolite analysis) to characterize the physiological response to *n*-butanol exposure in *E. coli* with the idea that the results would be useful for improving the tolerance of *n*-butanol producers. Cell-wide studies of microbial production hosts have been used in the past to optimize synthesis of a variety of products, ranging from primary metabolites to pharmaceutical compounds, and this is a well-reviewed topic (28, 31).

Solvent stress from aliphatic alcohols and alkanes has been studied in a variety of bacteria. While the trend is an increase in toxicity with an increase in solvent hydrophobicity, the mechanism of toxicity varies with the length of the carbon backbone (2). In general, the toxicity of the alcohol correlates well with the octanol-water partition coefficient, P_{ow} (2); at saturating concentrations, solvents with a log P_{ow} greater than 3.8 are not toxic to *E. coli*. The degree of toxicity of an alcohol also varies across bacteria, with some bacteria being more affected by the length of the alkyl chain while others are more affected by saturation (fewer double bonds) (22). Most toxicity studies have proposed the cell membrane as the most affected target of organic solvents and a significant factor in adapting to the stress. Both long- and short-chain alcohols are known to cause stress by either desiccation (short) or by intercalating in the hydrophobic cell wall fatty acids (long) (19, 20, 22) and may be critical factors in the robustness of a host microbe during fuel production. *n*-Butanol stress has been studied in solventogenic *Clostridia*, where toxicity was primarily ascribed to the chaotropic effects of the solvent (5), and it was hypothesized that expression of chaperones would alleviate stress caused by solvent exposure. In *Clostridium acetobutylicum*, transcript analysis after exposure to 0.75% *n*-butanol indicated that the primary response was accumulation of transcripts encoding chaperones, proteases, and other heat shock-related proteins (45), and overexpression of the GroELS chaperones produced strains with greater *n*-butanol tolerance (46). In *E. coli*, stress from ethanol exposure is the most widely studied alcohol stress

* Corresponding author. Mailing address: Physical Biosciences Division, Lawrence Berkeley National Laboratory, 1 Cyclotron Rd., MS 978-4121, Berkeley, CA 94720. Phone: (510) 495-2628. Fax: (510) 486-4252. E-mail: amukhopadhyay@lbl.gov.

† Supplemental material for this article may be found at http://aem.asm.org/.

▽ Published ahead of print on 29 January 2010.

‡ The authors have paid a fee to allow immediate free access to this article.

(18), and knowledge from cell-wide stress response studies has been applied to create better ethanologenic hosts (3). Recent studies have examined the effect of isobutanol in *E. coli*, where transcript analysis revealed several key mechanisms including the disruption of quinone function and the involvement of global regulators such as ArcA (7).

In this study, we characterized the response of *E. coli* to exogenous *n*-butanol stress using transcript and protein analyses. Several important candidates were further examined using the corresponding Keio collection mutants (4) to examine their involvement in *n*-butanol tolerance. Additional experiments such as quantitative PCR measurements and metabolite and reactive oxygen species (ROS) assays were used to follow-up on key results. Results from these experiments provide the criteria to select mechanisms that are the ideal targets for host engineering efforts.

MATERIALS AND METHODS

Culture conditions. For toxicity assays, *Escherichia coli* DH1 (ATCC 33849) was grown from freezer stocks in LB or M9 minimal medium with additional trace elements (32). To determine the effect of *n*-butanol on *E. coli* DH1 growth, a wide range of concentrations were tested first (data not shown) and then narrowed to a range that caused stress but not significant cell death. Growth assays to test the effect of different concentrations of *n*-butanol on *E. coli* DH1 were performed in 250-ml baffled shake flasks with 30 ml of M9 medium and a 2% inoculation from an overnight culture shaken at 200 rpm at 37°C. Unless noted otherwise, all subsequent *n*-butanol stress assays were conducted at 0.8% (vol/vol) *n*-butanol. pH was also measured for 0.8% *n*-butanol-exposed and control cultures.

For microarrays and proteomics experiments, cultures were grown in 1-liter shake flasks containing 300 ml of M9 medium shaking at 200 rpm. *n*-Butanol was added to a final concentration of 0.8% at mid-log phase (optical density at 600 nm [OD_{600}], 0.35 to 0.4/ml), and biomass was collected at the time points indicated in Tables 1 and 2. The cultures were centrifuged (10,000 × *g*, 4°C, 5 min), and cell pellets were immediately frozen in liquid nitrogen and stored at −80°C.

Gene deletion mutants were obtained from the Keio collection (4). The wild-type strain for the Keio deletion strains, BW2550, was obtained from the CGSC collection (http://cgsc.biology.yale.edu). Strains were adapted and tested in M9 medium using 24-well microtiter plates at 37°C using a plate reader (Safire; Tecan). Gas-permeable plate covers (PlateMax Ultraclear sealing film; Axygen Scientific, CA) were applied after addition of *n*-butanol.

Microarray sample preparation. For microarray samples, total RNA was isolated using the RNeasy Midi kit (Qiagen). RNA quality and quantity were measured with a Bioanalyzer (Agilent Technologies, Santa Clara, CA) and NanoDrop ND-1000 spectrophotometer (NanoDrop Technologies, Wilmington, DE), respectively. Reverse transcription reactions were performed as described previously (25). RNA in the reactions was hydrolyzed with 100 mM NaOH–10 mM EDTA at 65°C for 10 min and neutralized in 500 mM HEPES, pH 7.0. The remaining Tris in the cDNA suspension was removed by washing with water three times in a Microcon-YM30 (Millipore, Billerica, MA). The solutions were concentrated with a SPD2010 SpeedVac system (Thermo Scientific, Waltham, MA) prior to labeling with Alexa fluorophores (555 and 647) (Invitrogen, Co., Carlsbad, CA). Labeled cDNA was purified using Qiaquick PCR columns (Qiagen, Germantown, MD) and dried again in a SPD2010 SpeedVac system. The samples were rehydrated in Slide Hyb 3 (Invitrogen Co., Carlsbad, CA), and samples from each time point (stressed and control) were pooled together prior to hybridization.

E. coli microarrays were prepared by spotting 70-mer oligonucleotides (Eurofins MWG Operon, Huntsville, AL) onto Superamine 2 substrates (Arrayit Co., Sunnyvale, CA) using a robotic spotter (Digilab, Inc., Holliston, MA) (38). One oligomer representing each open reading frame (ORF) was spotted in triplicate on the slide. A prehybridization was performed with 5× saline-sodium citrate (SSC)–0.2% sodium dodecyl sulfate (SDS)–1% bovine serum albumin (BSA) for 60 min at 42°C. Hybridization was carried out at 42°C for 17 h, and the hybrids were washed subsequently with 1× SSC–0.2% SDS at 42°C, 0.1× SSC–0.2% SDS at 25°C, and 0.1× SSC at 25°C, all for 2 min at medium agitation in a hybridization station (Tecan). Three replicate hybridizations were performed for each time point from the three biological replicate pools of RNA.

Microarray data analysis. Hybridized slides were scanned at a 10-μm resolution with a GenePix 4200A microarray scanner (MDS Analytical Technologies, Sunnyvale, CA) at 70% laser power. Images were analyzed using GenePix Pro (MDS Analytical Technologies, Sunnyvale, CA) to globally normalize fluorescence intensity for each spot in both channels. Relative expression levels for each spot were calculated by dividing the intensity of the stressed sample by the intensity of the control sample. Local hybridization and intensity-dependent artifacts across the arrays were removed by Loess normalization using the Standardization and Normalization of Microarray Data (SNOMAD) program (8). The final log ratio for each gene was calculated by averaging the three replicate spots on each slide and the average ratio from the three biological replicate slides. *z*-scores for each gene were calculated using the formula

$$z = \frac{\log_2(\text{stress/control})}{\sqrt{0.25 + \Sigma\ \text{variance}}}$$

where 0.25 is a pseudovariance (30). Ratios with $\log_2 > |2|$ and *z*-score $> |1.96|$ were considered significant. Complete data are available at http://www.microbesonline.org/cgi-bin/microarray/viewExp.cgi?expId=1319 (1) and via the NCBI's Gene Expression Omnibus (11) (GEO series accession no. GSE16973). MicrobesOnline was also used to examine the raw data in terms of genes with similar functions and metabolic pathways.

Proteomics sample preparation. The volume of cells collected was based on the in-solution digestion protocol described previously to ensure isolation of approximately 1 mg of total protein for analysis (37). Cell pellets were washed in 1 M phosphate-buffered saline (pH 7) and flash frozen in liquid nitrogen. The cells were then lysed in a buffer containing 6 M urea and 500 mM triethylammonium bicarbonate, which provides denaturing conditions and is compatible with iTRAQ tag labeling. Protein concentration was determined using the Bio-Rad protein assay kit (Bio-Rad, Hercules, CA), and samples were prepared for iTRAQ labeling as described previously (37). Briefly, protein samples were reduced using Tris-2-carboxyethylphosphine, blocked using iodoacetic acid, and proteolysed using trypsin. Samples were then labeled with isobaric iTRAQ tags as per the manufacturer's protocol (Applied Biosystems, Foster City, CA). iTRAQ tags were used as follows: 114:T1, stress; 115:T2, control; 116:T1, control; and 117:T2, stress.

Two-dimensional liquid chromatography-tandem mass spectrometry. Strong cation exchange fractionation was completed using high-performance liquid chromatography as described previously (37). Electrospray ionization quadrupole time-of-flight mass analyzers (QSTAR Hybrid Quadrupole TOF and QSTAR Elite; Applied Biosystems, Foster City, CA) were used for sample analysis. Generally, 40 μl of each sample was injected using an Ultimate high-performance liquid chromatograph with Famos autosampler and Switchos micro column switching module onto a PepMap100 trapping column (0.3 by 5 mm) (Dionex, Inc., Sunnyvale, CA). Reverse-phase separation was completed on a C_{18} column (75-μm inside diameter) at a flow rate of 200 nl/min using an acetonitrile (ACN)-formic acid (FA) gradient buffer system: A, 2% ACN–0.1% FA; and B, 98% ACN–0.1% FA. Ions in the range of 350 to 1,600 *m/z* with a charge state of 2+ to 4+ were scanned for and selected. Ions were required to exceed a threshold of 50 counts to be selected as parent ions for fragmentation. Parent ions and their isotopes were excluded from further selection for 60 s. The instrument was manually calibrated and tuned following each batch of 2 to 4 samples. A digest of BSA was used as a standard to evaluate system performance.

Proteomics data analysis. Collected mass spectra were analyzed using ProteinPilot (Applied Biosystems, Foster City, CA). A FASTA file containing all the open reading frame (ORF) protein sequences of *E. coli*, obtained from NCBI, was used to generate the theoretical search database. Data analysis was conducted as described previously (37). Only proteins identified by at least two unique peptides at greater than 95% confidence were considered confidently identified and used for further analysis. To determine if a ratio was statistically significant, a standard score (z) was used, $z = (x - \mu)/\rho$, where x is the value of the individual protein ratio, μ is the population mean, and ρ is the population standard deviation. For protein ratios exposed to 1 h of *n*-butanol stress, μ was −0.037 and ρ was 0.65. For protein ratios exposed to 2 h of *n*-butanol stress, μ was −0.0042 and ρ was 0.34. In general, ratios with *z*-scores $\geq |1.5|$ were considered as significantly changed. Complete proteomics data are provided in Table S1 in the supplemental material.

qPCR. Total RNA for quantitative reverse transcriptase PCR (qPCR) was extracted as described for microarray analysis. An additional DNase treatment was performed on 10 μg of total RNA with Turbo DNase (Ambion). A total of 3.2 μg treated total RNA was reverse transcribed with 2 μg random hexamers

TABLE 1. Selected microarray data

COG category and gene name[a]	Log_2 stress/control ratio at:				Additional COG category
	Prestress	30 min	80 min	195 min	
COG C					
cyoA	0.76	−0.24	2.66	2.14	C
cyoB	1.10	−0.92	2.69	1.44	C
cyoC	0.51	−0.53	2.26	1.70	C
cyoD	0.93	−0.31	1.94	1.13	C
cyoE	0.56	−0.49	1.47	0.65	O
nfsA	0.33	2.10	1.17	1.21	C
nuoA	0.61	1.29	0.57	1.82	C
nuoB	0.68	1.29	0.98	1.61	C
nuoC	0.37	0.59	1.79	1.63	C
nuoE	0.53	0.67	1.29	1.40	C
nuoF	0.77	0.47	1.59	1.98	C
nuoG	0.82	0.65	1.87	2.23	C
nuoH	0.14	0.56	1.80	1.86	C
nuoI	0.34	0.49	2.02	2.02	C
nuoJ	0.07	0.42	1.65	1.35	C
nuoK	0.13	0.47	1.75	1.89	C
nuoL	0.06	0.20	0.97	1.04	CP
nuoM	0.10	0.25	1.59	1.03	C
nuoN	0.10	0.38	1.83	0.79	C
sdhC	0.45	−0.63	2.04	1.90	C
sdhD	0.19	−1.14	0.69	0.19	C
sdhA	0.63	−1.76	1.35	0.84	C
sdhB	0.92	−1.43	1.10	0.56	C
yqhD	−0.29	2.63	0.99	0.65	C
COG E					
cysD	−0.15	−2.07	−0.41	−0.32	E
dcp	0.21	−0.31	0.26	−0.09	E
gadA	−1.62	−0.64	−0.11	0.30	E
glnH	−0.20	0.17	−0.90	−1.55	ET
hisI	−0.22	−0.08	−1.27	−1.04	E
leuD	1.22	−2.35	−3.17	−0.76	E
metE	−0.30	−3.83	−4.16	−3.90	E
oppA	0.40	2.45	0.60	1.45	E
oppB	0.35	2.45	1.40	1.70	EP
oppC	0.14	2.16	1.85	1.47	EP
oppD	−0.12	2.36	2.00	1.22	EP
oppF	−0.05	2.32	1.78	1.16	E
potF	−0.50	−0.62	−0.61	−0.88	E
COG G					
malE	1.14	4.02	−1.34	−1.01	G
manX	0.76	2.67	0.55	2.26	G
manY	0.66	2.72	0.63	1.76	G
mgsA	−0.06	0.22	−0.91	−0.53	G
COG J					
raiA	1.06	2.05	−0.62	2.57	J
rmf	−1.19	3.22	2.84	1.96	J
rplB	1.00	−2.07	−1.11	−0.94	J
rplD	1.19	−2.19	−0.89	−0.64	J
rplS	0.50	−1.88	−2.02	−1.94	J
rplW	1.03	−2.11	−0.90	−0.73	J
yhbH	−0.12	0.97	0.05	−0.17	J
COG M					
acrA	0.05	1.23	1.41	0.11	M
acrB	0.37	1.73	2.33	0.75	V
ompF	1.76	−5.18	−4.07	−1.95	M
tolC	0.13	0.04	−0.15	0.31	MU
COGs O and P					
clpB	−1.05	1.04	0.40	0.82	O
cpxP	0.33	2.70	4.47	2.76	UNTP
cyoE	0.56	−0.49	1.47	0.65	O
dnaJ	−0.32	0.71	0.16	−0.23	O
groELS	0.09	1.04	0.41	−0.53	O
groS	0.10	0.78	0.28	0.34	O
htpG	−0.13	0.72	0.28	−0.50	O
htrA	0.13	1.71	1.10	0.45	O
ibpA	−0.56	0.26	−0.64	−0.04	O
ibpB	−0.56	0.76	−0.52	−0.16	O
katG	0.09	0.00	−0.57	−1.01	P
sodA	0.34	−0.61	1.98	0.64	P
sodC	−0.67	−0.08	0.46	−0.20	P
spy	−0.28	2.63	2.67	1.84	UNTP
yegD	0.75	−0.89	2.01	−1.92	O
COG T					
arcA	−0.25	−0.22	−1.14	−0.01	TK
cpxA	−0.16	−0.08	−0.31	−0.86	T
cpxR	−0.17	−0.77	−0.64	−0.88	TK
evgA	0.26	1.22	0.59	0.84	TK
evgS	0.11	2.14	2.83	1.73	T
phoB	0.14	1.19	0.88	0.49	TK
phoR	−0.73	0.38	0.39	0.06	T
Additional uncategorized genes					
asr	−1.15	5.31	3.41	2.47	
crl	0.24	−0.20	−0.26	0.00	
marA	−0.13	2.92	1.14	0.43	

[a] COG C, energy production and conversion; COG E, amino acid transport and metabolism; COG G, carbohydrate transport and metabolism; COG J, translation, ribosomal structure, and biogenesis; COG M, cell wall, membrane, and envelope biogenesis; COG O, posttranslational modification, protein turnover, and chaperones; COG P, inorganic ion transport and metabolism; COG T, signal transduction mechanisms.

TABLE 2. qPCR stress/control ratios for selected genes

Gene	Log_2 stress/control ratio for gene at[a]:					
	0 min	5 min	30 min	80 min	185 min	260 min
cyoA	−0.33	**−5.25**	−1.41	−0.83	**2.60**	**3.82**
cpxP	−0.82	**5.04**	**3.44**	**3.29**	**3.08**	**2.49**
rpoH	−0.24	1.02	1.03	0.65	**−2.63**	−1.50
ompF	−0.15	**−4.71**	**−6.29**	**−6.69**	−1.99	−1.98
evgS	−0.66	0.31	0.17	1.53	**3.86**	1.55
marA	−0.05	**2.76**	**2.75**	1.90	1.15	1.80
arcA	−0.16	−1.86	−0.27	−0.94	−1.82	−1.12

[a] Genes with a log_2 stress/control ratio of >2 are in bold.

and SuperScript III (Invitrogen) for 3 h at 50°C. The cDNA product was treated with RNase H (Invitrogen) and diluted 25-fold for quantitative PCR. The primers used for qPCR are listed in the supplemental material (see Table S1). qPCR was performed on the StepOnePlus instrument (Applied Biosystems) using 1 μl of diluted cDNA as template in 25-μl reactions with the DyNamo HS SYBR green Supermix (Finnzymes) and 0.2 μM each of the primers. Fold change in expression of target genes was calculated relative to the control samples. The primers used are provided in Table S2 in the supplemental material.

Reactive oxygen species assay. Control and *n*-butanol-stressed *E. coli* cultures were grown in M9 medium as described with various concentrations of *n*-butanol. To 5 ml of fresh M9 medium, 100 μl of each overnight culture was added, and then 140 μl of this diluted culture was transferred into a 96-well plate and incubated at 37°C for 45 min. As per the manufacturer's instruction, positive controls for oxidative stressed cells were prepared by adding 10 μl of 7.78 M *tert*-butyl hydroperoxide (TBHP) (Invitrogen, Co., Carlsbad, CA) to one set of control cells before incubation. Ten microliters of 25 mM 5 (and 6-)-carboxy-

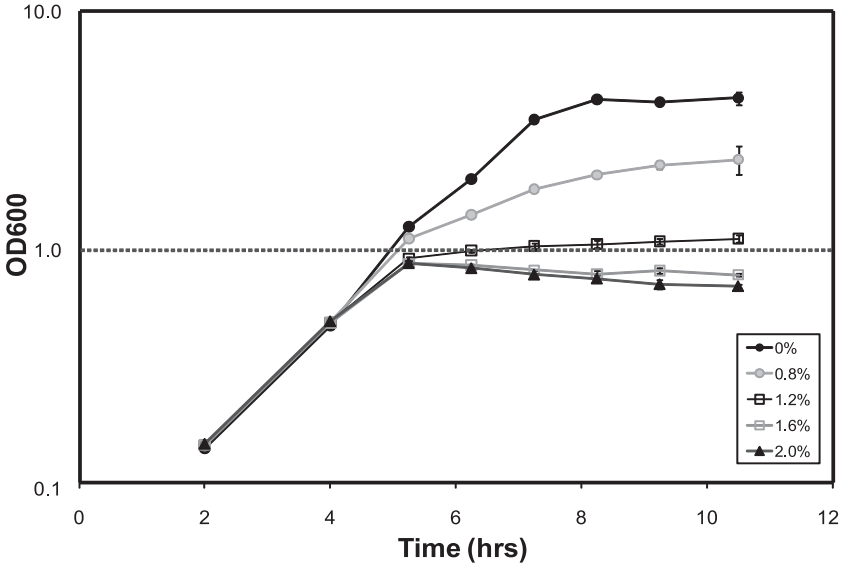

FIG. 1. Growth of *E. coli* DH1 in M9 minimal medium in the presence of various concentrations (vol/vol) of *n*-butanol. *n*-Butanol was added in mid-log phase (OD_{600} of ~0.35/ml, 4 h after subculture).

2′,7′-dichlorodihydro-fluorescein diacetate (carboxy-H_2DCFDA) was added to all cells. Florescence at 535 nm and optical density at 600 nm were measured for 45 min at 5-min intervals after adding dye using a plate reader (Safire, Tecan Infinite 200). Specific fluorescence is $[A_{535}/A_{600}]$.

RESULTS AND DISCUSSION

Toxicity tests. The range of *n*-butanol concentrations found to be inhibitory to *E. coli* DH1 in this study (Fig. 1) is consistent with trends noted in the literature for alcohol toxicity in *E. coli* (20). The concentration of *n*-butanol that caused a 50% growth decrease in M9 medium was found to be 0.8% (vol/vol) and was selected for the other growth assays and functional genomic analyses in this study. The pH of control cultures decreased from 7.0 at the start of the assay to 6.1 in stationary phase. However, in cultures exposed to 0.8% *n*-butanol, the pH decreased to 5.3 in stationary phase. The significance of this pH change will be discussed later.

Functional-genomics analysis. The temporal response at the transcript level showed 82 genes to be significantly changed at 30 min, 63 genes at 80 min, and 32 genes at 195 min. To obtain a broad overview of changes, the significantly changing transcripts were viewed in terms of the cluster of orthologous genes (COG) to which they belong. A COG consists of individual orthologous genes or orthologous sets of paralogs. Since orthologs often have the same function, it allows transfer of functional information from one member to an entire COG and provides the framework for functional genome analysis (44). In *E. coli*, 3,862 of 4,502 genes have COG descriptions. Distributing the significantly changing transcripts into their respective COG categories revealed the most perturbed categories to be energy production and conversion (C), amino acid transport and metabolism (E), and signal transduction (T) (see Fig. S1 and S2 in the supplemental material).

Corresponding experiments using similar conditions were conducted for analysis of the proteome. A total of 1,336 proteins were identified at a 95% confidence interval from 55,900 distinct peptides from 103,904 spectra. Of these 997 were identified using 2 or more unique high-confidence peptides. The iTRAQ ratios were generated as described in Materials and Methods (see Table S1 in the supplemental material) and correlated well across the two time points (see Fig. S3 in the supplemental material). Comparison of changes at the transcript and proteomic levels showed good agreement for most significantly changing candidates (Fig. 2). To analyze the data, the identified proteins were also categorized into their respective COG categories; a selected list is shown in Table 2. The following sections present and discuss the results for key stress response groups observed using these functional-genomics analyses.

Responses in energy metabolism and oxidative stress mechanisms. Candidates categorized in COG C (energy conserva-

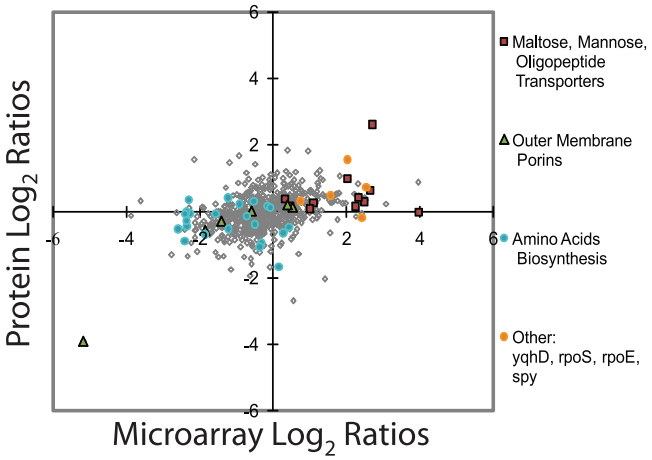

FIG. 2. Scatter plot of $\log_2$ ratios of transcript-level changes at 80 min versus the protein level at 60 min. The sets of most up- and downregulated candidates from both data sets are indicated.

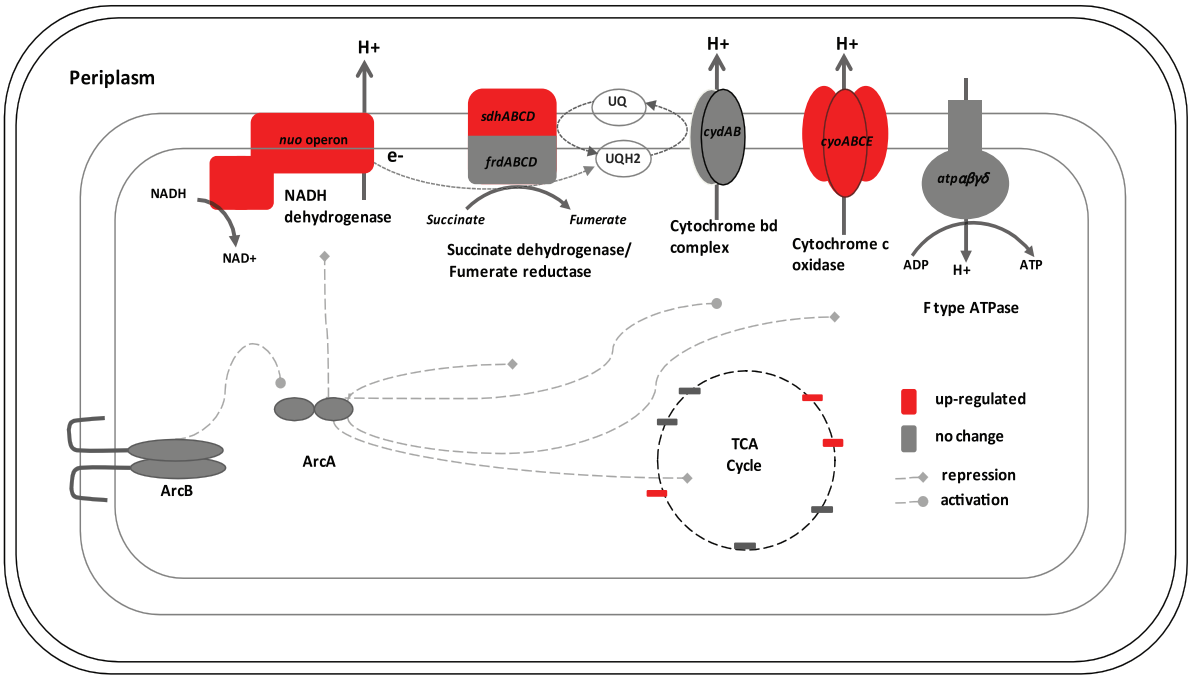

FIG. 3. Schematic model of microarray data for genes categorized with function in respiratory complexes and energy conservation are shown at 80 min after *n*-butanol exposure. The candidates depicted are energy metabolism complexes involved in oxidative phosphorylation in the KEGG pathway map (http://www.genome.jp/kegg/) and other ArcA-regulated genes.

tion and production) represented one of the main groups of significantly differentially expressed genes. Among these, two main sets of genes with changes in expression were observed: the 13-member *nuo* operon and the 5-member *cyo* operon (Table 1). The *nuo* operon encodes the NADH ubiquinone oxidoreductase (complex I), a multisubunit enzyme that couples electron transfer from NADH to ubiquinone with the translocation of protons across the cytoplasmic membrane and forms an integral part of oxidative phosphorylation (17) (Fig. 3). The concerted increase in the transcript levels of all members of this complex across all time points after exposure to *n*-butanol suggests an increased requirement for energy or a disruption in the respiratory efficiency of the organism. The latter has been proposed to occur in the eukaryote *Saccharomyces cerevisiae* during alcohol stress due to increased membrane fluidity causing dissipation of H^+ potential (41). Impact of *n*-butanol exposure on membrane-related function, including the inability to maintain an optimal pH gradient, has also been reported in *Clostridium acetobutylicum* (6). Increases in the transcripts in the *cyo* operon, which encodes a terminal oxidase (the cytochrome b_{562}-*o* complex), and *sdh* genes, which encode the succinate dehydrogenase complex, both involved in oxidative phosphorylation (17) (Table 1 and Fig. 3), also indicate a perturbation in respiratory balance. This cytochrome complex is known to be responsive to redox changes caused by increased permeability of the cell wall (9). Interestingly, the *cyo* and *nuo* operons were reported to be downregulated during isobutanol stress after 10 min of exposure (7). qPCR analysis of the *cyoA* indicated a decrease in transcript levels at early time points and an increase at later time points (Table 2) consistent with both results. Protein changes reflected many of the changes also seen in the microarrays for COG C, including significant upregulation in CyoB. All members of the *nuo* operon were identified via proteomics, and the NuoB subunit protein levels increased significantly during *n*-butanol exposure. The remaining proteins encoded by the *nuo* operon (NuoCEFG, NuoI, and NuoK) increased or showed no change across both time points. Other significantly increased proteins in this category were an NADPH-dependent, flavin mononucleotide (FMN)-dependent nitroreductase, NfsA (Table 3).

The upregulation in the *cyo*, *nuo*, and *sdh* operons over time were accompanied by several other significant changes, such as the upregulation of *sodA*, encoding a superoxide dismutase, and *yqhD*, encoding an alcohol dehydrogenase, suggesting an oxidative stress response. The proteomics data identified several candidates known to be part of bacterial antioxidant stress responses (42). The levels of many of these proteins, such as YqhD, also showed significant increases (Table 3).

The results at the transcript and protein level suggested a disruption of respiratory mechanisms and oxidative stress, often caused by an increase in intracellular reactive oxygen species (ROS). To compare the intracellular ROS levels of control and *n*-butanol-exposed cultures, cells were labeled with carboxy-H_2DCFDA, a known fluorogenic marker for ROS *in vivo*. Cells exposed to increasing levels of *n*-butanol showed increasingly elevated levels of fluorescence (Fig. 4). This result agrees with the measurements at the transcript and protein levels, and taken together, these findings indicate an oxidative stress in *E. coli* in response to *n*-butanol exposure (Fig. 5).

Responses in amino acid metabolism and metabolite transport. COG E (amino acid transport and metabolism) contained the most downregulated genes (see Fig. S1 and S2 in the supplemental material). Downregulation in several genes related to histidine, leucine, arginine, tryptophan, and methio-

TABLE 3. iTRAQ proteomics $\log_2$ ratios for select protein candidates

COG category and protein name[a]	$\log_2$ stress/control ratio at[b]:		Additional COG category
	60 min	120 min	
COG C			
CyoB	1.68	0.26	C
CydA	0.34	0.92	C
NfsA	0.91	0.91	C
NuoB	1.01	0.07	C
NuoE	0.23	0.06	C
NuoF	0.20	0.12	C
NuoG	−0.05	0.06	C
NuoI	0.31	−0.02	C
NuoK	0.14	0.92	C
YqhD	0.73	0.81	C
COG E			
CysD	−1.22	−0.73	E
GadA	−1.92	−1.28	E
GlnH	−1.68	0.25	ET
HisJ	−0.62	−0.47	E
LeuD	−0.45	−0.84	E
OppA	0.54	0.81	E
OppD	0.42	0.45	EP
OppF	0.15	0.63	E
PotF	−1.58	−0.12	E
COG G			
MalE	−0.04	0.75	G
ManX	0.63	0.86	G
ManY	2.61	0.88	G
MgsA	0.48	0.86	G
COG J			
RaiA	1.56	1.18	J
RplB	−0.34	−0.41	J
RplD	−0.94	−0.59	J
RplS	−0.51	−0.42	J
RplW	1.56	−0.59	J
YhbH	1.82	0.89	J
COG M			
AcrA	0.06	0.26	M
AcrB	0.51	0.19	MV
OmpF	−3.91	−1.79	M
TolC	−0.23	0.33	MU
COGs O and P			
ClpB	0.58	0.44	O
CpxP	0.97	0.68	UNTP
GroEL	0.58	0.20	O
GroS	0.48	0.22	O
IbpB	0.79	−0.03	O
KatG	0.12	0.30	P
SodA	−0.47	−0.01	P
SodB	0.25	0.09	P
SodC	−0.14	0.43	P
Spy	−0.19	0.96	O
Additional uncategorized protein			
Crl	−1.22	−0.73	

[a] COG C, energy production and conversion; COG E, amino acid transport and metabolism; COG G, carbohydrate transport and metabolism; COG J, translation, ribosomal structure, and biogenesis; COG M, cell wall, membrane, and envelope biogenesis; COG O, posttranslational modification, protein turnover, and chaperones; and COG P, inorganic ion transport and metabolism.

[b] For the corresponding standard *z*-scores, see Table S1 in the supplemental material.

nine biosynthesis and transport was observed (Table 1). Consistent with the transcript data, significant decreases in protein levels were also seen, including histidine (HisJ), cysteine (CysD), leucine (LeuD), glutamine (GlnH), glutamate (GadA), and putrescine (PotF) metabolism or transport (Table 3). The only prominently upregulated genes in this category were members of the *opp* operon (*oppABCDF*) that encodes a polyamine-induced oligopeptide ABC transport system. OppAFD proteins were also highly upregulated (Table 3). This Opp oligopeptide transport system was also reported to be upregulated in response to isobutanol exposure (7). The upregulation in the Opp system suggests a role of polyamines in *n*-butanol stress. Polyamines (e.g., putrescine and spermidine) are known to play an important role during acid stress (50), and the pH lowering in the butanol-stressed cultures is within the range known to elicit an acid stress response (10, 43). However, several polyamine production and transport systems are known in *E. coli* and form part of this category, and no other polyamine-related candidate showed significant change (for complete data see the microarray URL).

Based on the transcript and protein data, the levels of several metabolites known to be involved in both osmotic and acid stress were measured using capillary electrophoresis-mass spectrometry (CE-MS) (see Fig. S5 in the supplemental material). These included several amino acids, osmoprotectants, and amino acid-derived compounds. Consistent with the downregulation in both biosynthetic and utilization pathways, the levels of most metabolites measured were found to be lower or remained unchanged in *n*-butanol exposed cells (Fig. S5). Glutamate, alanine, and glycine were the most abundant amino acids in both control and stressed samples, but their levels were significantly reduced in the stressed samples relative to those in control samples. *n*-Butanol has been reported to cause a chaotropic effect in *Clostridium* strains (6), and amino acids such as glutamate are known osmoprotectants and also known to play a role in acid stress (10). To examine if supplementation of medium with the most highly accumulated amino acids (glutamate and alanine) could mitigate the growth effect of *n*-butanol exposure, *E. coli* DH1 cultures were grown in a defined medium containing *n*-butanol and amino acids at levels reported in osmoprotection assays in the literature (30). However, the addition of no single amino acid or combination of amino acids alleviated the growth impact imposed by *n*-butanol exposure substantially (see Fig. S6 in the supplemental material). Hence, while it is possible that *n*-butanol exposure created a stress similar to the chaotropic effect described for *Clostridium*, there does not appear to be any impact of osmoprotecting amino acids on growth during *n*-butanol exposure.

Extracytoplasmic stress and heat shock responses. The *cpx* genes *cpxR* and *cpxP* were the two most upregulated genes during *n*-butanol stress in *E. coli* (COG T) (Table 1). The CpxR/A two-component system responds to protein degradation and cell envelope stresses (21). Correspondingly, other members of this regulon, *cpxP* and *degP*, were among the most highly upregulated genes in this stress (Table 1). The upregulation of the *cpxP* transcript was confirmed using qPCR (Table 2). Also upregulated was the transcript encoding the envelope stress protein *spy*. CpxP and Spy were also among the most significantly increased proteins during *n*-butanol stress (Table 3). In addition to the envelope stress response, upregulation was also observed in genes encoding chaperones (e.g., *dnaJ*

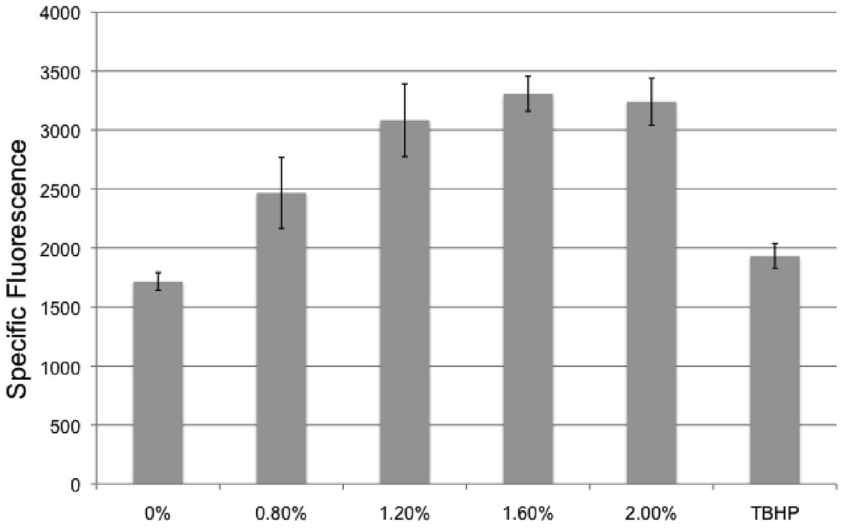

FIG. 4. Measurement of intracellular reactive oxygen species using carboxy-H_2DCFDA. The *n*-butanol concentrations used (vol/vol) are as indicated. "TBHP" represents control cells treated with *tert*-butyl hydroperoxide, which is known to produce intracellular H_2O_2 and which served as a positive control. The data shown are fluorescence measured after 15 min of treatment with carboxy-H_2DCFDA. Measurements were conducted in triplicate. For complete data, see Fig. S4 in the supplemental material.

and *htpG*) and proteases (e.g., *clpB*) at both the transcript and protein levels (Tables 1 and 3). The proteomics data set included other proteins associated with heat shock (IbpAB) and envelope stress (Table 3). These changes suggest the involvement of heat shock and protein-misfolding responses modulated as part of the σ^H and σ^E regulons during *n*-butanol exposure. σ^H (encoded by *rpoH*) is the well-studied heat shock regulator known to primarily regulate the cytoplasmic heat stress response (13). σ^E (encoded by *rpoE*) is typically found to be involved in response to extracytoplasmic (or cell envelope) and extreme heat stress, but it has also been shown to control a large number of cytoplasmic genes, including *rpoH* (15).

Though several members of the σ^H regulon were upregulated after exposure to *n*-butanol, *rpoH* itself showed only a small upregulation (Tables 1 and 2). σ^H has been established to be a major response factor during exposure to 10% ethanol (49), and the involvement of σ^H-regulated genes in *n*-butanol stress is not surprising. Furthermore, heat shock responses have been documented not only in general stress but also specifically during *n*-butanol stress in other organisms (45). In contrast to *rpoH*, *rpoE* showed a strong upregulation at 30 min after *n*-butanol exposure (Table 1). Upregulation in the *cpx* genes and the increase in σ^E strongly suggest cell envelope stress (Fig. 5). Consistent with the involvement of σ^E, several transcripts encoding outer membrane proteins—for example, the outer membrane protein porin F (*ompF*)—were significantly downregulated (Tables 1 and 2). Interestingly, the transcript encoding RseA, the primary negative regulator of σ^E, was also significantly upregulated (Table 1).

Carbohydrate transport and metabolism. Several proteins in COG G (carbohydrate transport and metabolism), particularly those associated with the membrane or located in the periplasm, showed increased levels in response to *n*-butanol stress (Tables 1 and 3). *manX* and *manY*, encoding the mannose phosphotransferase system, were highly upregulated at both the transcript and protein levels. This system transports and phosphorylates exogenous hexoses (mannose, glucose, fructose, etc.) and releases the phosphate esters into the cytoplasm (36). The *manXYZ* system has also been implicated in solvent tolerance in *E. coli* (33). Interestingly, another upregulated protein, MgsA (methylglyoxal synthase), limits the accumulation of phosphorylated sugars and has been postulated to provide a bypass mechanism for triose phosphate metabolism during growth in inadequate inorganic phosphate levels (47). The transcript levels of the maltose ABC transporter, specifically the periplasmic maltose-binding protein MalE, increased noticeably at early time points. MalE is documented to have chaperone-like properties such as interacting with unfolded or denatured proteins and preventing aggregation under heat shock conditions (38). However, while many of these systems have been functionally characterized in *E. coli*, the significance of their change during *n*-butanol exposure requires further investigation.

Additional stress responses. Changes in candidates in the COG T category (signal transduction systems) suggested the involvement of other stress response mechanisms during *n*-butanol exposure (Table 1 and Fig. 5). Specifically, *evgS*, which encodes the sensor protein of the EvgS/EvgA two-component system, was highly upregulated. The upregulation of the *evgS* transcript was confirmed using qPCR (Table 2). The EvgS/EvgA system is known to control a broad set of genes and plays a central role during acid resistance, osmotic adaptation, and drug resistance. This two-component system is known to effect the regulation of a variety of efflux pumps (12). Consistent with the upregulation in *evgS*, the genes *acrB*, which encodes part of the AcrA/B-TolC multidrug efflux system, and *marA*, which also encodes part of an efflux pump system, which are widely documented to be involved in solvent resistance (3, 34), were among the most upregulated genes (Tables 1 and 2). Though not greater than a $\log_2$ of |2|, the *phoB*/*R* transcripts were also found to be upregulated. PhoB/R is documented to regulate the small RNA-encoding *asr* as part of the acid stress response

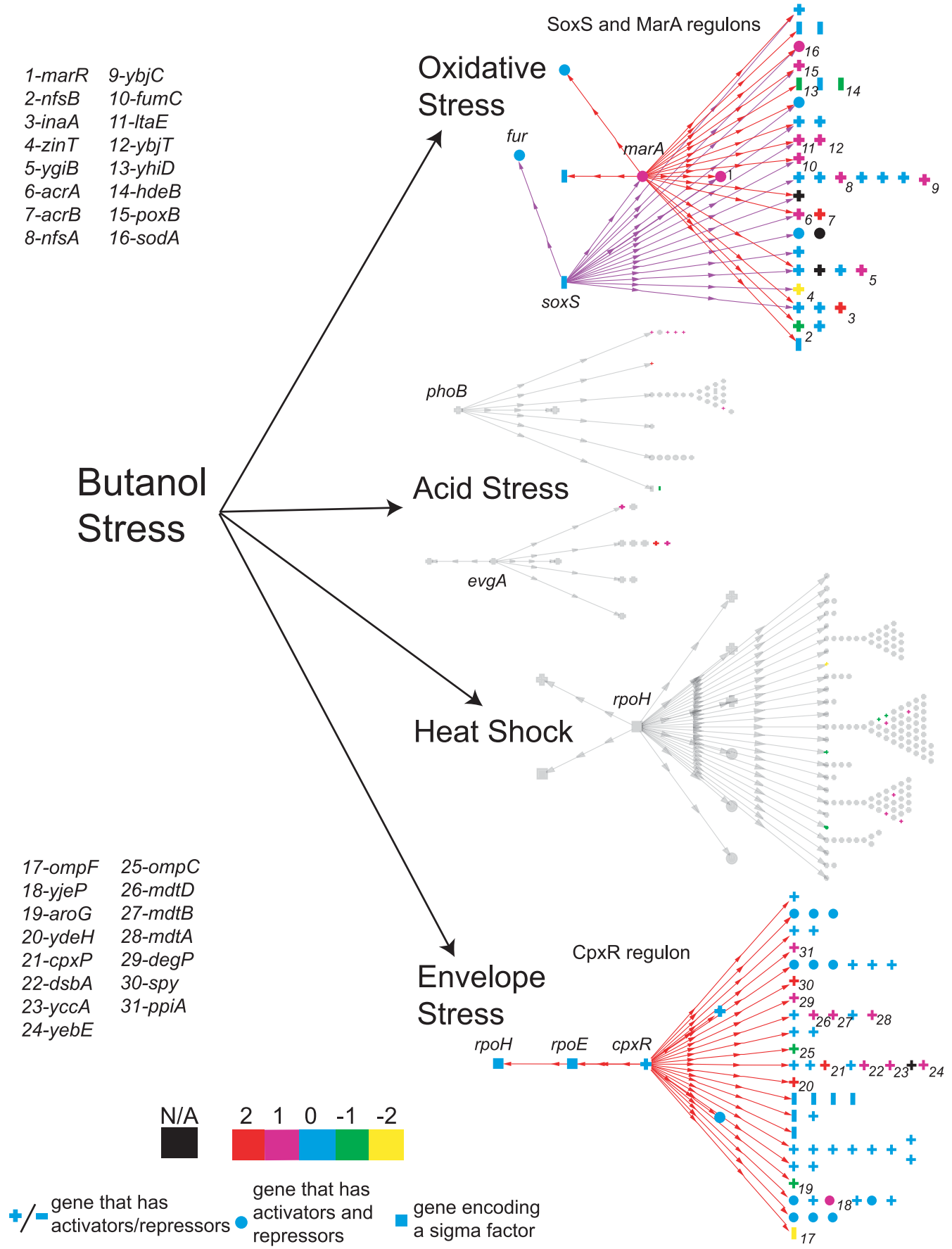

(40). The *asr* transcript is known be upregulated in *E. coli* in pH ranges from 4.0 to 5.0 (43) and was highly upregulated across all time points sampled after *n*-butanol exposure (Table 1 and Fig. 5).

Changes were also observed in several ribosomal protein-encoding genes (Table 1). RaiA (29), a translation inhibitor during cold shock, showed upregulation at both the transcript and protein levels. Also highly upregulated was YhbH, which has high sequence similarity to RaiA (29). Although not assigned to a COG category, Crl has been shown to regulate the activity and abundance of the RNA polymerase component σ^S (48) and was downregulated during *n*-butanol stress.

Examination of knockout mutants. The functional-genomics survey presented several interesting candidates that may be targeted for future host engineering. Changes at the transcript or protein levels for these candidates can potentially contribute to stress mitigation in *E. coli* or may be caused as a result of the stress. One tool for exploring the role of such candidates is the Keio collection of single-gene deletion strains (4). The *E. coli* base strain of the Keio collection (BW25113) is different from the *E. coli* strain used in this study (DH1) but was found to have similar relative resistance to *n*-butanol (Table 4; see Fig. S7 in the supplemental material). The similarity in responses of BW25113 and DH1 to *n*-butanol stress justified use of selected gene deletion mutants from the Keio collection to assess the impact of these genes on *n*-butanol sensitivity. Deletion strains were selected to include candidates that showed no differential expression (*dcp* and *mobB*), upregulation (*cpxP*, *envY*, *sodC*, and *malE*), and downregulation (*envY*, *metE*, and *ompF*) during *n*-butanol exposure (Table 4). Selected strains were grown with and without the addition of 0.8% *n*-butanol and compared with the wild-type background. The strains lacking envelope stress regulators *cpxP* and *envY* showed minimal growth impairment during *n*-butanol exposure. The Δ*metE* strain showed better growth with *n*-butanol exposure than the wild type at later stationary phase, consistent with the observations in the transcript, protein, and metabolite data and suggesting that the system preferentially downregulates methionine production during *n*-butanol stress. The Δ*malE*, Δ*yqhD*, and Δ*ompF* mutants showed increased sensitivity to *n*-butanol exposure at the 4-h time point, while the Δ*evgS* and Δ*malE* strains demonstrated the poorest growth at later time points. The additional sensitivity suggests that these genes may play a beneficial role in *n*-butanol stress and may provide some relief if overexpressed in an engineered host. It should be noted that despite the growth impact, such as that seen for Δ*yqhD*, Δ*evgS*, Δ*ompF*, and Δ*malE*, all of the strains tested showed at least moderate growth in the presence of *n*-butanol, indicating that the mitigating role provided by these genes is not essential, but rather part of a larger set of mechanisms.

Conclusions. Exposure to alcohols has been reported to impact bacterial growth via a variety of mechanisms, including increased membrane fluidity, ion leakage, changes in fatty acid composition, difficulties in translation, and elongation of cells (5, 6, 18, 19, 22, 27, 41, 45). Results from this study indicate that *n*-butanol exposure leads to a combination of several responses including cell envelope stress, oxidative stress, perturbation in respiratory systems, protein misfolding, acid stress, and induction of efflux systems (Fig. 5). With significant changes in several respiratory and oxidative stress proteins, the oxidative stress mechanism appears to be one of the strongest responses during *n*-butanol exposure. The increase in intracellular ROS levels in the *n*-butanol-exposed cells further confirmed these observations. The functional-genomics data also suggest a strong cell envelope stress.

These candidates, with highly correlated changes at the transcript and protein levels, may be potential engineering targets to generate stress-resistant hosts for fuel production, as they may also assist in stress relief during endogenous *n*-butanol production. The importance of several of these candidates was further emphasized by additional *n*-butanol sensitivity shown by the corresponding gene deletion strains. Specific genes, such as those encoding chaperones, have been reported to relieve up to 85% of the growth decrease caused by the addition of *n*-butanol in *Clostridium* (46) and based on our results may prove to be a valuable approach in *E. coli* as well. Similar relief may be provided via expression of redox stress response enzymes such as SodA and YqhD, both of which have also been reported for use in relieving growth defects due to oxidative stresses (23, 35).

In addition to cellular engineering, solvent adaptation, such as that used for *Pseudomonas putida* adapted to grow in up to

TABLE 4. Growth response of select gene deletion strains in *E. coli* DH1 (0.8% *n*-butanol exposure)

Strain[a]	Mean difference (SE) in OD_{600}/ml at[b]:	
	4 h	10 h
DH1	0.13 (0.01)	0.47 (0.04)
BW25113	0.26 (0.04)	0.48 (0.05)
Δ*dcp*	0.19 (0.01)	0.59 (0.04)
Δ*mobB*	0.24 (0.03)	0.29 (0.06)
Δ*evgS*	0.13 (0.00)	0.75 (0.05)
Δ*cpxP*	0.060 (0.02)	0.38 (0.01)
Δ*malE*	0.34 (0.01)	0.62 (0.03)
Δ*oppA*	0.23 (0.02)	0.33 (0.06)
Δ*sodC*	0.13 (0.02)	0.34 (0.07)
Δ*yqhD*	0.34 (0.02)	0.44 (0.05)
Δ*envY*	0.022 (0.01)	0.36 (0.03)
Δ*metE*	0.22 (0.03)	0.27 (0.08)
Δ*ompF*	0.33 (0.01)	0.43 (0.03)

[a] Strains were obtained from the Keio Collection (Japan). The background strain for the Keio knockouts (BW25113) was obtained from the Yale culture collection.

[b] Difference [control (0% *n*-butanol) − stress (0.8% *n*-butanol)] in optical density (OD_{600}) for a given strain. The time points are post *n*-butanol addition. Assays were conducted in triplicate in 24-well plates using the Tecan Safire plate reader in M9 medium.

FIG. 5. Overview of the impact of *n*-butanol exposure on different *E. coli* stress regulons at 80 min. Colors indicate the $\log_2$ cutoff as per the legend. The directions of arrows indicate the genes directly regulated by the global regulators, where each column of symbols represents genes with a unique set of regulators. Pluses and minuses indicate genes that either activated or repressed, respectively. Circles are genes that have both activators and repressors. Squares represent the sigma factors. The figure was generated using Biocyc Pathway tools (SRI, Menlo Park, CA).

6% (vol/vol) *n*-butanol (39), may improve solvent resistance in host strains. Solvent adaptation often involves complex responses involving short- and long-term mechanisms. The adaptive responses of bacteria to different solvents are very similar and include a variety of mechanisms (16). The complexity of stress response is also evident in our results (Fig. 5), and engineering single genes may not sufficiently increase *n*-butanol tolerance. The use of global regulatory proteins, specifically RpoH, RpoE, and ArcA, may allow the modulation of entire stress regulons and more complex systems such as the NADH-ubiquinone oxidoreductase complex or the cytochrome complex. Such global approaches for trait selection have been conducted, including mutations in the *E. coli rpoA* gene for improved resistance to commercially important products including *n*-butanol (26). Recent studies also suggest a potential use of RNA chaperones such as Hfq to modulate the role of protein complexes such as the Opp system (15). In conclusion, while numerous candidates showed significant changes at the transcript level, additional systems level analysis and follow-up studies should allow a more rational approach for cellular engineering of *E. coli* for an improved host platform for *n*-butanol production.

ACKNOWLEDGMENTS

We thank Vivek Mutalik and Mario Ouellet for helpful discussions, Edward Baidoo for advice on CE-MS protocols, Jason Baumohl and Marcin Joachimiak for help with uploading data to MicrobesOnline, and Pramila Tamrakar for help with growth assays.

This work was part of the Joint BioEnergy Institute supported by the U.S. Department of Energy, Office of Science, Office of Biological and Environmental Research, through contract DE-AC02-05CH11231 between Lawrence Berkeley National Laboratory and the U.S. Department of Energy.

REFERENCES

1. **Alm, E. J., K. H. Huang, M. N. Price, R. P. Koche, K. Keller, I. L. Dubchak, and A. P. Arkin.** 2005. The MicrobesOnline web site for comparative genomics. Genome Res. **15:**1015–1022.
2. **Aono, R., and H. Nakajima.** 1997. Organic solvent tolerance in *Escherichia coli*. Tanpakushitsu Kakusan Koso **42:**2532–2541.
3. **Asako, H., H. Nakajima, K. Kobayashi, M. Kobayashi, and R. Aono.** 1997. Organic solvent tolerance and antibiotic resistance increased by overexpression of *marA* in *Escherichia coli*. Appl. Environ. Microbiol. **63:**1428–1433.
4. **Baba, T., T. Ara, M. Hasegawa, Y. Takai, Y. Okumura, M. Baba, K. A. Datsenko, M. Tomita, B. L. Wanner, and H. Mori.** 2006. Construction of *Escherichia coli* K-12 in-frame, single-gene knockout mutants: the Keio collection. Mol. Syst. Biol. **2:**2006.0008.
5. **Baer, S. H., H. P. Blaschek, and T. L. Smith.** 1987. Effect of butanol challenge and temperature on lipid composition and membrane fluidity of butanol-tolerant *Clostridium acetobutylicum*. Appl. Environ. Microbiol. **53:**2854–2861.
6. **Bowles, L. K., and W. L. Ellefson.** 1985. Effects of butanol on *Clostridium acetobutylicum*. Appl. Environ. Microbiol. **50:**1165–1170.
7. **Brynildsen, M. P., and J. C. Liao.** 2009. An integrated network approach identifies the isobutanol response network of *Escherichia coli*. Mol. Syst. Biol. **5:**277.
8. **Colantuoni, C., G. Henry, S. Zeger, and J. Pevsner.** 2002. SNOMAD (Standardization and NOrmalization of MicroArray Data): web-accessible gene expression data analysis. Bioinformatics **18:**1540–1541.
9. **Cotter, P. A., V. Chepuri, R. B. Gennis, and R. P. Gunsalus.** 1990. Cytochrome o (*cyoABCDE*) and d (*cydAB*) oxidase gene expression in *Escherichia coli* is regulated by oxygen, pH, and the *fnr* gene product. J. Bacteriol. **172:**6333–6338.
10. **Diez-Gonzalez, F., and Y. Karaibrahimoglu.** 2004. Comparison of the glutamate-, arginine- and lysine-dependent acid resistance systems in *Escherichia coli* O157:H7. J. Appl. Microbiol. **96:**1237–1244.
11. **Edgar, R., M. Domrachev, and A. E. Lash.** 2002. Gene Expression Omnibus: NCBI gene expression and hybridization array data repository. Nucleic Acids Res. **30:**207–210.
12. **Eguchi, Y., T. Oshima, H. Mori, R. Aono, K. Yamamoto, A. Ishihama, and R. Utsumi.** 2003. Transcriptional regulation of drug efflux genes by EvgAS, a two-component system in *Escherichia coli*. Microbiology **149:**2819–2828.
13. **Erickson, J. W., V. Vaughn, W. A. Walter, F. C. Neidhardt, and C. A. Gross.** 1987. Regulation of the promoters and transcripts of *rpoH*, the *Escherichia coli* heat shock regulatory gene. Genes Dev. **1:**419–432.
14. **Ezeji, T. C., N. Qureshi, and H. P. Blaschek.** 2007. Bioproduction of butanol from biomass: from genes to bioreactors. Energy Biotechnol. Environ. Biotechnol. **18:**220–227.
15. **Guisbert, E., V. A. Rhodius, N. Ahuja, E. Witkin, and C. A. Gross.** 2007. Hfq modulates the sigmaE-mediated envelope stress response and the sigma32-mediated cytoplasmic stress response in *Escherichia coli*. J. Bacteriol. **189:**1963–1973.
16. **Heipieper, H. J., G. Neumann, S. Cornelissen, and F. Meinhardt.** 2007. Solvent-tolerant bacteria for biotransformations in two-phase fermentation systems. Appl. Microbiol. Biotechnol. **74:**961–973.
17. **Ingledew, W. J., and R. K. Poole.** 1984. The respiratory chains of Escherichia coli. Microbiol. Rev. **48:**222–271.
18. **Ingram, L. O.** 1990. Ethanol tolerance in bacteria. Crit. Rev. Biotechnol. **9:**305–319.
19. **Ingram, L. O.** 1986. Microbial tolerance to alcohols—role of the cell membrane. Trends Biotechnol. **4:**40–44.
20. **Ingram, L. O., and T. M. Buttke.** 1984. Effects of alcohols on microorganisms. Adv. Microb. Physiol. **25:**253–300.
21. **Isaac, D. D., J. S. Pinkner, S. J. Hultgren, and T. J. Silhavy.** 2005. The extracytoplasmic adaptor protein CpxP is degraded with substrate by DegP. Proc. Natl. Acad. Sci. U. S. A. **102:**17775–17779.
22. **Kabelitz, N., P. M. Santos, and H. J. Heipieper.** 2003. Effect of aliphatic alcohols on growth and degree of saturation of membrane lipids in *Acinetobacter calcoaceticus*. FEMS Microbiol. Lett. **220:**223–227.
23. **Kang, Y. S., Y. Lee, H. Jung, C. O. Jeon, E. L. Madsen, and W. Park.** 2007. Overexpressing antioxidant enzymes enhances naphthalene biodegradation in *Pseudomonas sp.* strain As1. Microbiology **153:**3246–3254.
24. **Keasling, J. D., and H. Chou.** 2008. Metabolic engineering delivers next-generation biofuels. Nat. Biotechnol. **26:**298–299.
25. **Kizer, L., D. J. Pitera, B. F. Pfleger, and J. D. Keasling.** 2008. Application of functional genomics to pathway optimization for increased isoprenoid production. Appl. Environ. Microbiol. **74:**3229–3241.
26. **Klein-Marcuschamer, D., C. N. Santos, H. Yu, and G. Stephanopoulos.** 2009. Mutagenesis of the bacterial RNA polymerase alpha subunit for improvement of complex phenotypes. Appl. Environ. Microbiol. **75:**2705–2711.
27. **Knoshaug, E. P., and M. Zhang.** 2009. Butanol tolerance in a selection of microorganisms. Appl. Biochem. Biotechnol. **153:**13–20.
28. **Lee, S. Y., D. Y. Lee, and T. Y. Kim.** 2005. Systems biotechnology for strain improvement. Trends Biotechnol. **23:**349–358.
29. **Maki, Y., H. Yoshida, and A. Wada.** 2000. Two proteins, YfiA and YhbH, associated with resting ribosomes in stationary phase *Escherichia coli*. Genes Cells **5:**965–974.
30. **Mukhopadhyay, A., Z. He, E. J. Alm, A. P. Arkin, E. E. Baidoo, S. C. Borglin, W. Q. Chen, T. C. Hazen, Q. He, H. Y. Holman, K. Huang, R. Huang, D. C. Joyner, N. Katz, M. Keller, P. Oeller, A. Redding, J. Sun, J. Wall, J. Wei, Z. M. Yang, H. C. Yen, J. Z. Zhou, and J. D. Keasling.** 2006. Salt stress in *Desulfovibrio vulgaris* Hildenborough: an integrated genomics approach. J. Bacteriol. **188:**4068–4078.
31. **Mukhopadhyay, A., A. M. Redding, B. J. Rutherford, and J. D. Keasling.** 2008. Importance of systems biology in engineering microbes for biofuel production. Curr. Opin. Biotechnol. **19:**228–234.
32. **Neidhardt, F., P. Bloch, and D. Smith.** 1974. Culture medium for enterobacteria. J. Bacteriol. **119:**736–747.
33. **Okochi, M., M. Kurimoto, K. Shimizu, and H. Honda.** 2007. Increase of organic solvent tolerance by overexpression of *manXYZ* in *Escherichia coli*. Appl. Microbiol. Biotechnol. **73:**1394–1399.
34. **Okusu, H., D. Ma, and H. Nikaido.** 1996. AcrAB efflux pump plays a major role in the antibiotic resistance phenotype of *Escherichia coli* multiple-antibiotic-resistance (Mar) mutants. J. Bacteriol. **178:**306–308.
35. **Perez, J. M., F. A. Arenas, G. A. Pradenas, J. M. Sandoval, and C. C. Vasquez.** 2008. *Escherichia* coli YqhD exhibits aldehyde reductase activity and protects from the harmful effect of lipid peroxidation-derived aldehydes. J. Biol. Chem. **283:**7346–7353.
36. **Postma, P. W., J. W. Lengeler, and G. R. Jacobson.** 1993. Phosphoenolpyruvate:carbohydrate phosphotransferase systems of bacteria. Microbiol. Mol. Biol. Rev. **57:**543–594.
37. **Redding, A., A. Mukhopadhyay, D. C. Joyner, T. C. Hazen, and J. D. Keasling.** 2003. Study of nitrate stress in *Desulfovibrio vulgaris* Hildenborough using iTRAQ proteomics. Brief. Funct. Genomic Proteomics **5:**133–143.
38. **Richarme, G., and T. D. Caldas.** 1997. Chaperone properties of the bacterial periplasmic substrate-binding proteins. J. Biol. Chem. **272:**15607–15612.
39. **Ruhl, J., A. Schmid, and L. M. Blank.** 2009. Selected *Pseudomonas putida* strains able to grow in the presence of high butanol concentrations. Appl. Environ. Microbiol. **75:**4653–4656.
40. **Seputiene, V., D. Motiejunas, K. Suziedelis, H. Tomenius, S. Normark, O. Melefors, and E. Suziedeliene.** 2003. Molecular characterization of the acid-inducible asr gene of *Escherichia coli* and its role in acid stress response. J. Bacteriol. **185:**2475–2484.

41. **Sikkema, J., J. A. M. Debont, and B. Poolman.** 1995. Mechanisms of membrane toxicity of hydrocarbons. Microbiol. Rev. **59:**201–222.
42. **Storz, G., and M. Zheng.** 2000. Oxidative stress, p. 47–59. *In* G. Storz and R. Hengge-Aronis (ed.), Bacterial stress responses. ASM Press, Washington, DC.
43. **Suziedeliene, E., K. Suziedelis, V. Garbenciute, and S. Normark.** 1999. The acid-inducible *asr* gene in *Escherichia coli*: transcriptional control by the *phoBR* operon. J. Bacteriol. **181:**2084–2093.
44. **Tatusov, R., N. Fedorova, J. Jackson, A. Jacobs, B. Kiryutin, E. Koonin, D. Krylov, R. Mazumder, S. Mekhedov, A. Nikolskaya, B. S. Rao, S. Smirnov, A. Sverdlov, S. Vasudevan, Y. Wolf, J. Yin, and D. Natale.** 2003. The COG database: an updated version includes eukaryotes. BMC Bioinformatics **4:**41.
45. **Tomas, C. A., J. Beamish, and E. T. Papoutsakis.** 2004. Transcriptional analysis of butanol stress and tolerance in *Clostridium acetobutylicum*. J. Bacteriol. **186:**2006–2018.
46. **Tomas, C. A., N. E. Welker, and E. T. Papoutsakis.** 2003. Overexpression of *groESL* in *Clostridium acetobutylicum* results in increased solvent production and tolerance, prolonged metabolism, and changes in the cell's transcriptional program. Appl. Environ. Microbiol. **69:**4951–4965.
47. **Totemeyer, S., N. A. Booth, W. W. Nichols, B. Dunbar, and I. R. Booth.** 1998. From famine to feast: the role of methylglyoxal production in *Escherichia coli*. Mol. Microbiol. **27:**553–562.
48. **Typas, A., C. Barembruch, A. Possling, and R. Hengge.** 2007. Stationary phase reorganisation of the *Escherichia coli* transcription machinery by Crl protein, a fine-tuner of sigma(s) activity and levels. EMBO J. **26:**1569–1578.
49. **VanBogelen, R., M. Acton, and F. Neidhardt.** 1987. Induction of the heat-shock regulon does not produce thermotolerance in *Escherichia coli*. Genes Dev. **1:**525–531.
50. **Yohannes, E., A. E. Thurber, J. C. Wilks, D. P. Tate, and J. L. Slonczewski.** 2005. Polyamine stress at high pH in *Escherichia coli* K-12. BMC Microbiol. **5:**59.